Field Demonstration of In-Line All-Optical Wavelength Conversion in a WDM Dispersion Managed 40-Gbit/s Link

D. Caccioli, Arianna Paoletti, Alessandro Schiffini, Andrea Galtarossa, *Senior Member, IEEE*, Paola Griggio, G. Lorenzetto, P. Minzioni, S. Cascelli, M. Guglielmucci, Luigi Lattanzi, Francesco Matera, G. M. Tosi Beleffi, V. Quiring, W. Sohler, Hubertus Suche, Samo Vehovc, and Matjaz Vidmar

***Abstract*—The development of wavelength-division multiplexing (WDM) all-optical transport networks is an interesting solution to increase the capacity of long-haul transmission systems and to solve the route-exhaust problems of metropolitan networks, driving down the cost of that traffic. Routing can be achieved using a transparent device able to select and interchange wavelengths, such as an all-optical wavelength converter. In this paper, an optical transport network over an embedded link located between Rome and Pomezia in Italy is emulated. The transmission has been realized along a WDM, 5 $\times$ 100 km long, dispersion managed link at 40 Gb/s. The in-line rerouting process has been controlled by means of an all-optical wavelength converter realized with a periodically poled lithium niobate waveguide. Moreover, a polarization-independent scheme for the converter has been exploited to allow the in-line signal processing. This scheme is based on the counterpropagation of TE and TM signal components along the same guide and results extremely compact.**

In this paper it is demonstrated that wavelength conversion and rerouting add no penalty with respect to the simple transmission along the embedded cable. This result seems to be another step toward the feasibility of true all-optical networks.

***Index Terms*—Field trial, 40 Gb/s, polarization, rerouting, wavelength conversion, wavelength-division multiplexing (WDM).**

I. Introduction

A CRUCIAL issue of network evolution is to meet the increasing bandwidth capacity at reduced cost [1]. A possible solution to fit this requirement can be found in the achievement of an all-optical network [2], [3]. An optical transport network (OTN) consists of the concatenation of optical devices and fiber links able to manage the optical information in a very dynamical way. An efficient solution to optimize the architecture of the OTN is wavelength-division multiplexing (WDM) [4], [5], which permits one to increase the potentiality of installed infrastructures. Moreover, WDM channels are very suitable for OTN where channels can be optically processed in the frequency domain by means of optical cross-connect nodes (OXCs). One possible device that can implement the functionality of an OXC node, i.e., extraction and reallocation of different channels, is an all-optical wavelength converter (AOWC) [6]. Extensive studies of wavelength-routed networks demonstrated that creating an OTN without AOWCs would imply a major waste of fiber bandwidth [7]. Moreover, wavelength converters simplify network management problem and enable ready interconnection between independently managed networks. Because of these considerations, it is straightforward that the main requirement for an AOWC is to be transparent to pulse length, modulation format, and signal bit rate. In particular, an ideal AOWC should be able to generate a converted signal without reducing signal power and optical signal-to-noise ratio (OSNR) level during the wavelength conversion process. Moreover, to be useful in WDM networks, the AOWC must allow the simultaneous conversion of several wavelengths. The aim of the IST-ATLAS (All-optical Terabit per second LAmbda Shifted transmission) Project has been to consider the issues of a point-to-point OTN, namely, what are the performance and the capacity of a connection and which are the requirements for OXC nodes. The main issue consisted in verifying the potentiality of rerouting process in high-bit-rate networks; therefore we chose to verify the AOWC performance over a WDM transmission link at 40 Gbit/s. Several experiments have already demonstrated the benefit, in terms of traffic, given by high-bit-rate WDM transmissions [8], [9].

In this paper, we present the experimental evaluation of an OTN, consisting of an embedded link WDM at 40 Gb/s with a switching-node based on wavelength conversion in a $LiNbO_3$ waveguide. The link used for the experiment is located between Rome and Pomezia, where both G.652 and G.655 fibers are deployed along a dispersion managed link. The total link length is 500 km, but after 300 km one of the WDM channels is dropped, converted by the AOWC to a different wavelength, and reinserted into the line to be propagated with the unconverted channels up to the end of the link. The description of the entire experiment is organized as follows: AOWC features are presented

Manuscript received October 10, 2003; revised February 20, 2004. This work was supported by the IST program under Contract IST-1999-10 626 (ATLAS Project).

D. Caccioli, A. Paoletti, and A. Schiffini are with Pirelli Laboratories, 20126 Milano, Italy.

A. Galtarossa, P. Griggio, and G. Lorenzetto are with the Department of Information Engineering, Università di Padova, 35131 Padova, Italy (e-mail: paola@wave.dei.unipd.it).

P. Minzioni is with INFM, Department of Electronics Engineering, Università di Pavia, 27100 Pavia, Italy.

S. Cascelli, M. Guglielmucci, and L. Lattanzi are with ISCTI, 00144 Rome, Italy.

F. Matera and G. M. Tosi Beleffi are with Fondazione Ugo Bordoni, 00142 Rome, Italy.

V. Quiring, W. Sohler, and H. Suche are with Fachbereich Physik, D-33098 Paderborn, Germany.

S. Vehovc and M. Vidmar are with University of Ljubljana, 25 1000 Ljubljana, Slovenia.

Digital Object Identifier 10.1109/JSTQE.2004.827838

in Section II; in Section III the line setup is described and critical aspects such as losses, chromatic dispersion compensation, and polarization-mode dispersion are discussed. Finally, in Section IV, results demonstrating the error-free channel rerouting without the aid of any error-correction code are reported.

II. Wavelength Converter

Several techniques to implement an AOWC have been studied and reported in the literature [10]. Usually, wavelength conversion experiments performed in communication systems exploit one of the following techniques: four wave mixing in highly nonlinear fibers (HNLFs), nonlinear effects in semiconductor optical amplifiers (SOAs), or parametric difference frequency generation in periodically poled lithium niobate waveguide (PPLN) [11].

The major problem given by the use of HNLFs is that the conditions assuring high conversion efficiency, i.e., high signal power and high nonlinear coefficient, enhance signal distortion because of self-and cross-phase modulation effects. This makes it very difficult to obtain a converted signal with a sufficiently high power not affected by strong distortions. The use of SOAs has some advantages with respect to HNLFs [12]; in particular signal power is not required to be particularly high, because the SOAs amplify the input signal during the conversion process. The main problem of this technique is that during conversion process a nonnegligible amplified spontaneous emission (ASE) power is generated together with converted signal, causing a reduction of the OSNR level. Furthermore, SOA conversion efficiency depends on signal bit-rate and pulse modulation format. Additionally, both signal and pump power must be carefully controlled to obtain low signal degradation, caused by nonlinear effects in the SOA, together with high conversion efficiency [13], [14].

The process of wavelength conversion based on parametric difference frequency generation in PPLN is very attractive, because its characteristics are quite close to those of an ideal AOWC. During the conversion process only negligible noise from spontaneous parametric fluorescence is added to a converted signal and no signal distortion is introduced. Moreover, the converter is transparent to signal bit-rate and modulation format, [10], [11] and allows high conversion efficiency [15]. In addition, the wavelength conversion bandwidth is broad (typically >50 nm), allowing multichannel conversion. Despite these advantages, PPLN suffers from the presence of the photorefractive effect [16]. One common solution to avoid photorefractive damage is to maintain the $LiNbO_3$ waveguide at high temperature, so that charges are easily removed from trap levels present in the crystal; thus, in our experiment the waveguide has been maintained around 200°. Nevertheless, this must not be considered a limit of PPLN applicability because some crystals, obtained by slightly doping $LiNbO_3$, show a strong reduction of photorefractive effect also at ambient temperature [17]. The development of such a PPLN-based waveguide will allow the operation of the AOWC at low temperatures as well.

A very promising technique to be used in the PPLN waveguides consists of combining the second-harmonic generation with the difference frequency generation in a single device (cascading technique) [18], [19]. In such a device a fundamental wave at frequency ω_f is used to generate a pump wave at frequency $\omega_p = 2\omega_f$. At the same time the pump wave interacts with a signal at frequency ω_s and generates the converted wave (also called "idler") at frequency $\omega_c = \omega_p - \omega_s = 2\omega_f - \omega_s$. The coherent process described above is polarization dependent, since phase-matching conditions are strongly affected by the polarization of the incoming signals. As a consequence, as the polarization is uncontrollable along a link, the in-line wavelength conversion may be really inefficient. In order to remove this drawback, many solutions have been proposed and demonstrated using a polarization diversity scheme, as reported in [19] and [20]. Generally, schemes proposed in the literature require identical phase-matching conditions in two different waveguides, and a compensation of the differential group delay accumulated by the two signal polarization components [20]. In this paper we introduce a novel scheme that allows one to use only one waveguide, so that identical phase-matching conditions are guaranteed between the two polarization components and equalization of the differential group delay between the two polarization components is automatically realized. In order to describe with accuracy the AOWC setup, first the characterization of a PPLN-waveguide is reported; subsequently the polarization-independent scheme that allows effective use of the PPLN-waveguide as an in-line converter is discussed in detail.

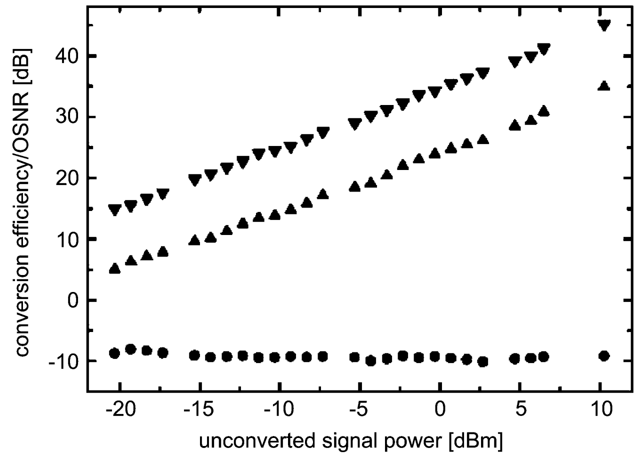

Fig. 1. Conversion efficiency and OSNR versus power of the unconverted signal for the PPLN-waveguide. The power of the fundamental wave (at 1557.36 nm) is constant and equals 22.4 dBm. The circles represent the conversion efficiency; the up- and down-triangles are the OSNR of the converted and unconverted signal, respectively. The OSNR figures are obtained with 0.1 nm of resolution bandwidth.

A. Characterization of the Wavelength Converter

The waveguide used during the field trial has been fabricated at Paderborn University by means of a titanium indiffusion on a PPLN crystal. To begin with, the conversion bandwidth of the device has been characterized: the 3-dB conversion bandwidth equals 55 nm. Another important issue regards the conversion efficiency of the device. Using a 22.4-dBm power of the fundamental wave at 1557.36 nm, the conversion efficiency (measured as the ratio of converted power to unconverted power at the output of the device) of −8 dB has been achieved. Results are reported in Fig. 1, where the OSNR figures are obtained with 0.1 nm of resolution bandwidth. As can be observed, the OSNR

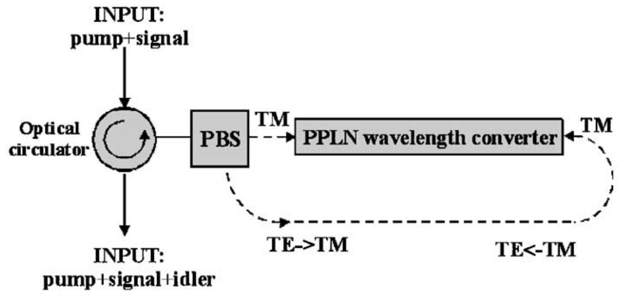

Fig. 2. Polarization-independent scheme for wavelength conversion. (PBS stands for polarization beam splitter.)

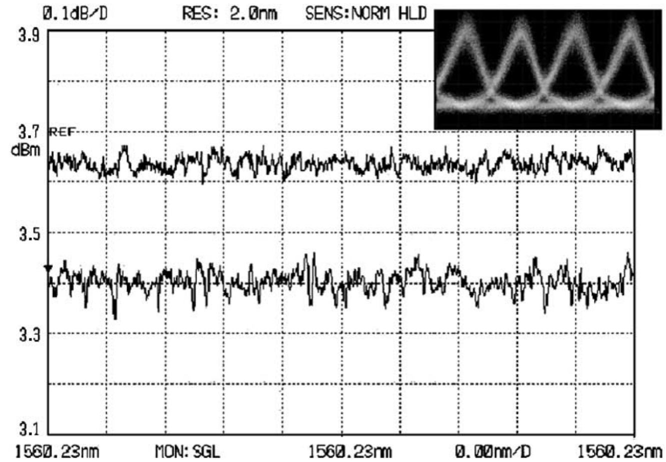

Fig. 3. Power fluctuation of the converted signal: the upper and lower trace represent the maximum and minimum value, respectively. Inset: the optical eye diagram of the converted signal during the polarization scrambling of the incoming radiation.

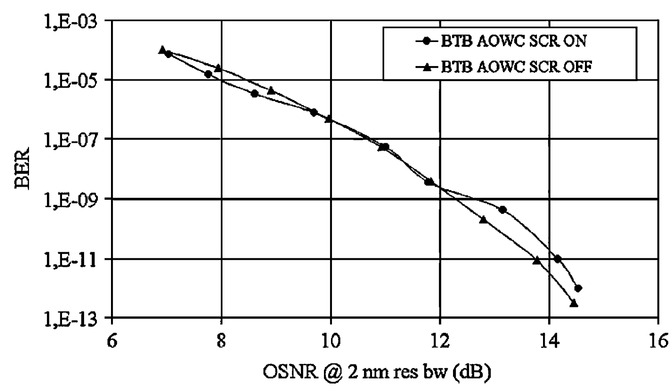

Fig. 4. BER measurement back-to-back for the PPLN-waveguide: the circles correspond to the scrambled signal; the triangles refer to the transmission without scrambling.

is completely determined by input OSNR of unconverted signal and by conversion efficiency. No measurable excess noise due to the conversion process itself could be detected. Within 30 dB power change of unconverted signal, the ratio between the signal and idler OSNR was exactly the conversion efficiency. Using an arrayed waveguide grating as narrow-band filter in front of the PPLN-wavelength converter, the out-of-band noise was removed, improving the effective OSNR of the converted signal of about 5 dB. In fact, filtering the input signal before the PPLN waveguide avoids adding spurious ASE noise in the wavelength region in which the idler is generated. If a multichannel wavelength conversion is realized, the efficiency of the process is slightly lower, around -10 dB (instead of -8 dB) over the 3-dB conversion bandwidth [15], [21]. Moreover, by switching individual channels, no change in efficiency has been observed, nor any difference measured between continuous-wave and pulsed signal. The insertion loss of the device is around 5 dB for TM polarization (and 3.5 dB for TE polarization).

B. Polarization-Independent Scheme

The polarization-independent scheme applied is particularly simple and compact, as shown in Fig. 2. Both fundamental wave and signal are independently amplified, filtered, and then combined by a 10(signal):90(fundamental) coupler into an optical circulator. The incoming radiation is divided into two components TE and TM by means of a polarization beam splitter (PBS). Subsequently, the light is launched into the guide according to a counterpropagating scheme. It is worth noting that the whole configuration is polarization maintaining (PM). The PM pigtail carrying the TE component of the signal is rotated by 90° and spliced to the right pigtail of the converter in order to guarantee TM coupling. In the same way, the converted signal corresponding to the TM component is rotated to TE and recombined with the TM idler component by the same PBS. With this scheme, adjusting the polarization state of fundamental wave, it is possible to control the fundamental power on the two branches of ring configuration, thus controlling the conversion efficiency of signal polarization components. Interference effects due to internal backreflections are reduced as much as possible by the AR-coating waveguide endfaces and by angled fiber to waveguide coupling. The most relevant advantage of this scheme consists in using a single guide. This assures identical phase-matching condition for both polarization components as well as the automatic compensation of the differential group delay between the two counterpropagating components of signal and idler. We notice that by means of the 90° rotated pigtail, any other polarization rotator device external to the guide has not been used.

In order to test the polarization independence of this scheme, a fundamental wave of 24 dBm has been fed into the circulator, and its polarization has been adjusted to obtain the same conversion efficiency for both TE and TM components of the incoming signal. Then a polarization scrambled signal has been fed into the AOWC, and variations of idler power have been recorded on an optical spectrum analyzer. By proper adjustment of fundamental wave polarization, it has been possible to achieve a -1 dBm idler signal at the output of wavelength converter, and idler power variations, observed in a long-term measurement, showed a polarization sensitivity of about 0.2 dB. Fig. 3 reports the idler power fluctuations during the polarization scrambling of the incoming signal. The figure is obtained using an optical spectrum analyzer (OSA) setting the span width at 0 nm, and the two traces represent the upper and lower limit of the power oscillation. The long-term optical eye diagram of converted channel is shown in the inset of Fig. 3. We confirmed the reliability of the proposed scheme also in terms of system performance by means of bit error rate (BER) measurement. In Fig. 4 the performance of converted channel, carrying a 40-Gbit/s stream

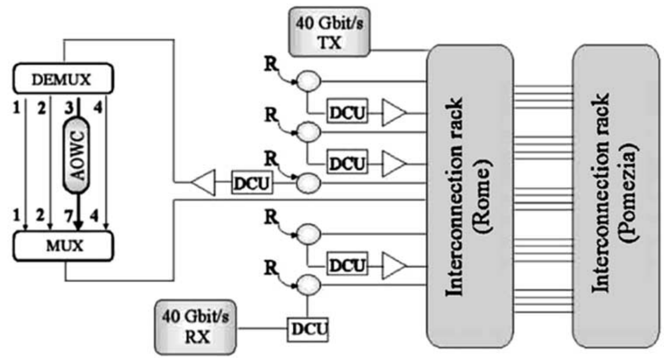

Fig. 5. Field trial setup between Rome and Pomezia (R: Raman amplifier, DCU: dispersion compensating unit).

	D_{SPAN} (ps/nm)	S_{SPAN} (ps/nm^2)	α_{SPAN} (dB)	PMD (ps/km$^{1/2}$)
G.655	240.33	6.12	23.9	0.06
DCF1	-239.43	-1.17	2.8	0.10
G.652	1542.76	5.34	22.2	0.03
DCF2	-1543.76	-3.99	12.4	0.13

Fig. 6. Main specifications of the two different fiber types with the corresponding dispersion compensating fibers (DCF) measured at the reference wavelength of 1552.52 nm. $D_{\mathrm{SPAN}}, S_{\mathrm{SPAN}}$, and α_{SPAN} stand for chromatic dispersion, chromatic dispersion slope, and attenuation per span, respectively; these are mean values measured over the 100-km spans that form the link. The last column reports the PMD coefficient, as usually given in ps/km$^{1/2}$.

of 5-ps full-width at half-maximum (FWHM) pulses, with and without the polarization scrambler, are compared. The reported OSNR has been measured by means of an OSA setting the resolution bandwidth at 2 nm. The results highlight that no additional penalty is introduced by the polarization scrambler.

III. Field Trial Setup

As we mentioned in the Introduction, we evaluated the performance of the previously described AOWC along a WDM embedded link at 40 Gbit/s. A scheme of trial setup is sketched in Fig. 5. The fibers are looped back four times to obtain about 100-km spans, and by repeating the same configuration five times, a 5×100 link has been reproduced. Due to the fact that in the cable both G.655 and G.652 are deployed, two links 500 km long over both kind of fibers were obtained. The transmitter–receiver as well as the optical amplifiers and the AOWC were located in the Rome site.

The transmitter consists of four DFB lasers in the C-band, at the wavelengths 1550.92, 1552.52, 1554.13, and 1555.75 nm, complying with the ITU-T wavelength grid. The multiplexed channels are externally modulated by two cascaded electroabsorption modulators (EAMs), providing pulse shaping and data encoding. Return-to-Zero (RZ) pulses 5-ps FWHM have been obtained by fine-tuning the first EAM bias voltage. It is worth noting that a low duty cycle has been used, according to results reported in [22], to reduce the impact of intrachannel nonlinear effects. On the receiver side, the channel has been demultiplexed, preamplified, filtered, and fed to both the clock recovery and the 40-Gbit/s electrical time-domain multiplexing receiver.

A. Link Specifications

Specifications regarding the fiber link are given in Fig. 6, where reported data correspond to the mean values per span at the reference wavelength 1552.52 nm. In the figure, $D_{\mathrm{SPAN}}, S_{\mathrm{SPAN}}$, and α_{SPAN} stand for chromatic dispersion, chromatic dispersion slope, and attenuation per span, respectively, whereas the last column reports the polarization-mode dispersion (PMD) coefficient, as usually given in ps/km$^{1/2}$. Main issues for the system performance concern optical amplification, chromatic dispersion compensation for each channel, and polarization mode dispersion impairment. Some details for each of them are given in the following sections.

1) Chromatic Dispersion Compensation: Chromatic dispersion has been compensated after each 100-km span by means of dispersion compensating units (DCUs). First, the dispersion management has been performed without the AOWC for the four propagating channels. The first-order compensation referred to the channel at 1552.52 nm was around 100%. The 200-GHz channel spacing induces taking into account also the dispersion slope of the fiber when other channels at 1550.92, 1554.13, and 1555.75 nm are considered. In the G.652 case, due to the lower slope value, only the first and fourth channels (1550.92 and 1555.75 nm) had to be adjusted in compensation: in fact, a proper amount of dispersion has been added at the receiver side, just after channel selection. Concerning G.655 fiber, the higher slope value involves the compensation of all three remaining channels.

2) Optical Amplification: Optical amplification has been realized following a hybrid scheme with both erbium-doped fiber amplifier (EDFA) and distributed Raman amplification. The choice of this hybrid scheme depends on the tradeoff between two effects. First, distributed Raman amplification provides advantages, in terms of noise figure, with respect to the EDFA; i.e., pure Raman amplification yields improvement of the OSNR with respect to pure double-stage EDFA amplification for the same system parameters [23]. On the other side, distributed Raman amplification can increase the nonlinear impairment due to the higher power of propagating signal [24]. This is the reason why we chose to amplify the signal by means of Raman amplification only along the 100 km spans and not through the DCUs, which are more sensitive to the nonlinear effects.

As mentioned, at the end of each span a counterpropagating 400-mW pump at 1455 nm has been inserted by means of an optical circulator to preamplify the signal before the DCU. The same power pump over two different kinds of fiber produces strongly different Raman gain values. Actually, the Raman effect produces 8 dB gain over G.652, whereas it provides 12 dB gain over G.655. After each compensation stage the radiation has been boosted through an EDFA to be repropagated along the following span. Due to the different fiber specifications, the output power of the in-line EDFA has been adjusted for each kind of fiber to ensure the best performance. More precisely, 3-dB dynamics, as aggregate power level, could be sustained in both cases, with $+15$ and $+13$ dBm as maximum boosted level from each EDFA for G.652 and G.655, respectively. Fig. 7

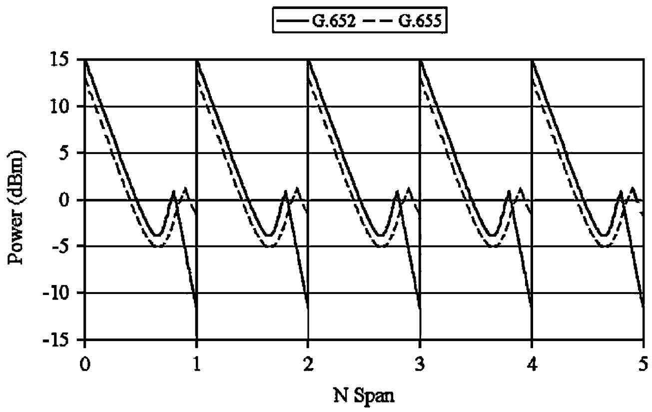

Fig. 7. Power budget management along the link. Solid and dashed lines correspond to G.652 and G.655 transmission, respectively.

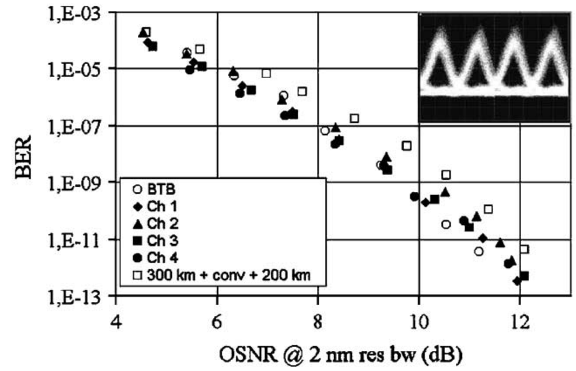

Fig. 8. BER versus OSNR (at 2-nm resolution bandwidth) of unconverted and converted channels (see legend) after 5×100 km of G.652 fiber, with $+6$ dBm mean optical power level per channel.

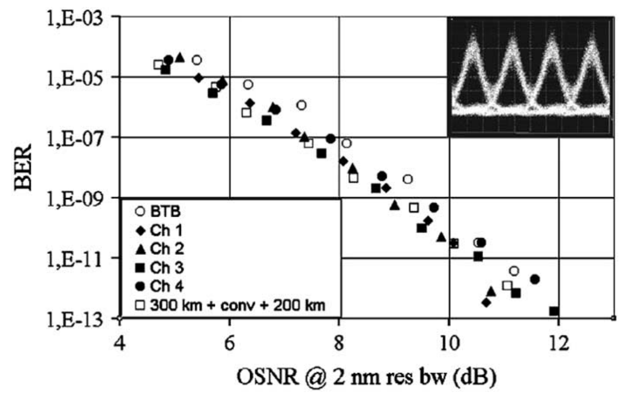

Fig. 9. BER versus OSNR (at 2-nm resolution bandwidth) of unconverted and converted channels (see legend) after 5×100 km of G.655 fiber, with $+4$ dBm mean optical power level per channel.

shows the obtained power map behavior along the link. The lower value of boosted power in the G.655 case is due to the enhanced nonlinear impairment [22], [25].

3) Polarization-Mode Dispersion (PMD) Effects: The embedded fibers have been characterized in terms of mean differential group delay (DGD) in two different moments. The first time, the measurements have been performed few months after the cable installation in 1996. The DGD was averaged over a 100-nm bandwidth around 1550 nm: the resulting PMD coefficient was 0.032 and 0.043 ps/$\sqrt{\text{km}}$ for G.652 and G.655 fibers, respectively. The link has been tested again during the year 2000 to evaluate the long-term DGD evolution. These measurements provided 0.032 and 0.061 ps/$\sqrt{\text{km}}$ as PMD coefficient for G.652 and G.655, respectively [26]. The mean DGD in G.655 fibers has increased in the last years, but the absolute value is still very low. By means of these measurements, and by means of a DCU characterization as reported in Fig. 6, the mean DGD value along the link can be estimated close to 1.14 and 1.38 ps for G.652 and G.655, respectively. Each EDFA adds around 0.2 ps, and therefore the overall mean DGD of the link gets close to 1.3 and 1.5 ps for G.652 and G.655, respectively. The average DGD per time slot ($T_{\text{slot}} = 25$ ps) in the worst case equals 6%. Considering this low value and the low duty factor of the propagated RZ pulses (around 20% of the time slot), we can affirm that in our experiment the PMD should have no impairment on the transmission performance [27]. This will be confirmed by experimental results.

IV. Experimental Results

During the field trial session, system performance has been analyzed in terms of BER curves versus OSNR with fixed optical input power in front of the 50-GHz photodiode. OSNR has been swept by remote controlling a variable optical attenuator (VOA) inserted just in front of the first EDFA at the receiver side. OSNR level with 2-nm resolution bandwidth was measured just after the same EDFA, i.e., before channel selection, with the maximum value corresponding to the line OSNR, which is straight determined by the power budget along the line.

In order to achieve less than 0.2 dB fluctuation on the input power level to the photodiode while sweeping OSNR within about 10 dB dynamic, we arranged three cascaded EDFAs plus an optical filter for each amplifier output. The first filter selects the channel to be measured with a 1.1-nm passband. The other two filters are 1.3-nm passband tunable filters, which are useful for cutting off the out-of-band optical noise contribution. In order to evaluate the performance of the OXC node along the link, a transmission of the four channels without the in-line AOWC has been deployed. Launching a 2^7-1 pseudorandom bit sequence length, all the channels stand within less than 1-dB penalty with respect to the back-to-back operation. It should be underlined that the measurements accuracy of our testbench is around 0.5 dB and that all the BER measurements reported in this letter have been performed without the aid of any error-correction code. In Fig. 8, we show the behavior of the BER versus OSNR for the G.652 transmission where the mean optical power per channel is around $+6$ dBm. Similar results are reported in Fig. 9 for G.655 fibers where the mean power per channel is $+4$ dBm. It is worth noting that all BER measurements presented in this paper have been performed at 10 Gbit/s but curves of all tributaries at 10 Gbit/s are not reported because they are almost superimposed.

Subsequently, the AOWC has been added after 300 km to convert the channel at 1554.13 nm into a new ITU wavelength at 1560.61 nm, using a 24-dBm power of fundamental wave at 1557.36 nm and thus generated pump wavelength at 778.68 nm. A proper amount of chromatic dispersion at the receiver side (just after the channel selection) has been added for the converted channel over both G.652 and G.655. First, for the propagation over G.652 fibers, the received optical eye diagram of the converted channel is reported in the inset of Fig. 8. The eye diagram obtained from converted channel is quite similar to that of the unconverted ones. This similar behavior is well confirmed by the BER measurements reported in Fig. 8. No evidence of penalty for the converted channel with respect to the unconverted ones has been found.

The same analysis has also been performed for transmission over G.655. In the inset of Fig. 9, the optical eye diagram of the converted channel at the receiver side is reported. Again, converted waveform does not present any anomalous shape with respect to the unconverted channels, and the wavelength conversion does not add penalty to the system without AOWC, as shown in Fig. 9.

V. Conclusion

In this paper, wavelength conversion and rerouting along an embedded link located between Rome and Pomezia has been demonstrated. The conversion has been realized by means of a PPLN all-optical wavelength converter. Thanks to a compact polarization-independent scheme, the AOWC has become more suitable for the transmission and the emulation of an OXC node. The field trial has been carried out over both G.652 and G.655 fibers along a 5×100 km WDM link operating at 40 Gbit/s. The excellent operation of this OXC node has been demonstrated without the aid of any error-correction code. This experiment seems to be another step toward the feasibility of the optical transport networks.

Acknowledgment

The authors would like to thank all the participants in the project without whom these results could not have been achieved: Opto Speed, Opto Speed Italia, Thomson-CSF, United Monolithic Semiconductors, University of Aveiro, and University College of London.

References

[1] R. Davey, D. Payne, and A. Lord, "Optical networks: A pragmatic european operator's view," in *Proc. OFC 2002*, Anaheim, CA, 2002.
[2] R. C. Alferness, "The all-optical networks," in *Proc. WCC-ICCT 2000*, Beijing, China, 2000.
[3] S. Barnes, "All optical networks: Principles, solutions, and challenges," in *Proc. OFC 2002*, Anaheim, CA, 2002.
[4] C. A. Brackett, "Dense wavelength division multiplexing networks: Principles and applications," *IEEE J. Select. Areas Commun.*, vol. 8, pp. 948–964, 1990.
[5] J. P. Blondel, "Massive WDM systems: Recent developments and future prospects," in *Proc. ECOC 2001*, Amsterdam, 2001.
[6] K.-C. Lee and V. O. K. Li, "A wavelength-convertible optical network," *J. Lightwave Technol.*, vol. 11, p. 962, 1993.
[7] M. Sabry and J. E. Midwinter, "Toward an optical aether," in *Proc. Inst. Elect. Eng. Optoelectron.*, vol. 14, 1994, pp. 327–335.
[8] Y. Frignac, G. Charlet, W. Idler, R. Dischler, P. Tran, S. Lanne, S. Borne, C. Martinelli, G. Veith, A. Jourdan, J. P. Hamaide, and S. Bigo, "Transmission of 256 wavelength division and polarization-division-multiplexed channels at 42.7 Gb/s (10.2 Tb/s capacity) over 3×1000 km of Teralight TM fiber," in *Proc. OFC 2002*, Anaheim, CA, 2002.
[9] B. Zhu, C. R. Doerr, P. G. L. Nelson, S. Stulz, L. Stulz, and L. Gruner-Nielsen, "72-nm continuos single-band transmission of 3.56 Tb/s (89×42.7 Gb/s) over 4000 km of NZDF fiber," in *Proc. ECOC 2003*, 2003.
[10] S. J. B. Yoo, "Wavelength conversion technologies for WDM network applications," *J. Lightwave Technol.*, vol. 14, pp. 955–966, 1996.
[11] M. H. Chou, I. Brener, M. M. Fejer, E. E. Chaban, and B. Christman, "1.55 μm band wavelength conversion based on cascaded second-order nonlinearity in $LiNbO_3$," *IEEE Photon. Technol. Lett.*, vol. 11, pp. 653–655, 1999.
[12] A. Schiffini, A. Paoletti, P. Griggio, P. Minzioni, G. Contestabile, A. D'Ottavi, and F. Martelli, "4×40 Gbit/s transmission in a 500 km long disperison-managed link, with in-line all-optical wavelength conversion," *Electron. Lett.*, vol. 38, pp. 1558–1560, 2002.
[13] A. D'Ottavi, F. Girardin, L. Graziani, F. M. Martelli, P. Spano, A. Mecozzi, S. Scotti, R. Dall'Ara, J. Eckner, and G. Guekos, "For wave mixing in semiconductor optical amplifiers: A practical tool for wavelength conversion," *J. Select. Topics Quantum Electron.*, vol. 3, pp. 522–528, 1997.
[14] J. Zhou, N. Park, K. J. Vahala, M. Newkirk, and B. Miller, "Four-wave mixing wavelength conversion efficiency in semiconductor traveling-wave amplifiers measured to 65 nm of wavelength shift," *IEEE Photon. Technol. Lett.*, vol. 6, pp. 984–987, 1994.
[15] H. Suche, G. Schreiber, Y. Lee, V. Quiring, R. Ricken, W. Sohler, A. Paoletti, F. Carbone, D. Caccioli, and A. Schiffini, "Efficient Ti:PPLN multiwavelength converter for high bit-rate transmission systems," in *Proc. ECOC 2001*, Amsterdam, the Netherlands, 2001.
[16] A. M. Glass, "The photorefractive effects," *Opt. Eng.*, vol. 17, pp. 470–479, 1978.
[17] T. R. Volk and M. Wohlecke, "Optical damage resistance in lithium niobate crystals," *Ferroelect. Rev.*, vol. 1, pp. 195–262, 1998.
[18] G. P. Banfi, P. K. Datta, V. Degiorgio, and D. Fortusini, "Wavelength shifting and amplification of optical pulses through cascaded second order processes in periodically-poled lithium niobate," in *Proc. CLEO/Eur. 1998*, Glasgow, Scotland, 1998.
[19] I. Cristiani, V. Degiorgio, L. Socci, F. Carbone, and M. Romagnoli, "Polarization-insensitive wavelength conversion in a lithium niobate waveguide by cascading technique," *IEEE Photon. Technol. Lett.*, vol. 14, pp. 669–671, 2002.
[20] I. Brener, M. H. Chou, M. Fejer, E. E.Chaban, K. R. Parameswaran, S. Kosinsky, and D. L. Pruitt, "Polarization-insensitive wavelength conversion based on cascaded nonlinearities in $LiNbO_3$," *Electron. Lett.*, vol. 36, pp. 66–67, 2000.
[21] H. Suche, Y. Lee, V. Quiring, R. Ricken, and W. Sohler, "All-optical wavelength conversion and switching in Ti:PPLN waveguides," in *Top. Meeting Photon. Switching 2002*, Korea, 2002.
[22] A. Pizzinat, A. Schiffini, F. Alberti, A. Paoletti, D. Caccioli, P. Griggio, P. Minzioni, and F. Matera, "Numerical and experimental comparison of dispersion compensation techniques on different fibers," *IEEE Photon. Technol. Lett.*, vol. 14, pp. 1415–1417, 2002.
[23] Y. Aoki, "Properties of fiber Raman amplifiers and their applicability to digital optical communication systems," *J. Lightwave Technol.*, vol. 6, pp. 1225–1239, 1988.
[24] A. Pizzinat, M. Santagiustina, and C. Schivo, "Impact of hybrid edfadistributed Raman amplification on a 4×40 Gb/s WDM optical communication system," *IEEE Photon. Technol. Lett.*, vol. 15, pp. 341–343, 2003.
[25] G. A. Agrawal, *Nonlinear Fiber Optics*. New York: Academic, 1995.
[26] A. Galtarossa, L. Palmieri, A. Pizzinat, M. Schiano, and T. Tambosso, "Measurement of local beat length and differential group delay in installed single-mode fibers," *J. Lightwave Technol.*, vol. 18, pp. 1389–1394, 2000.
[27] H. Sunnerud, M. Karlsson, C. Xie, and P. A. Andrekson, "Polarizationmode dispersion in high-speed fiber-optic transmission systems," *J. Lightwave Technol.*, vol. 20, pp. 2204–2219, 2002.

D. Caccioli, photograph and biography not available at the time of publication.

Arianna Paoletti was born in Livorno, Italy, in 1971. She graduated in telecommunications engineering from the Politecnico of Milan in 1997.

From 1998 to 2000 she was with the Optics Lab unit of the R&D department, Alcatel, in charge of the development of 10-Gb/s electrooptical interfaces. In 2000 she joined Pirelli Advanced Photonics Research group, dealing with the experimental investigations into high-speed (40–80 Gb/s) transmission systems. Since 2001 she has been with the WDM System Technology Laboratory, Pirelli Laboratories Optical Innovation.

Alessandro Schiffini was born in Ivrea (TO), Italy, in 1970. He received the physic degree from the University of Torino, Italy, in 1995.

In 1994, he joined Cselt Laboratories studying soliton mode-locked fiber lasers. In 1997, he joined Pirelli Cavi e Sistemi, working in the advanced photonics research group on high-speed transmission systems. His main areas of activity involve theory, design, and experimental investigation on high-bit-rate telecommunications systems and all-optical networks. In 2001, he joined the WDM System Technology Group, Pirelli Laboratories Optical Innovation.

Andrea Galtarossa (M'88–SM'03) received the degree in electronic engineering from the University of Padova, Padova, Italy, in 1984.

He received a postgraduate fellowship from Telettra Spa, Vimercate (IT), Italy, for research in wavelength-division multiplexing components in 1986. In 1990, he became an Assistant Professor in electromagnetic fields at the Department of Information Engineering, University of Padova. In 1998, he became an Associate Professor in microwave technology at the same university. He is author or coauthor of more than 80 papers. His current research activity is mainly in birefringent fibers and PMD measurements and modeling.

Paola Griggio was born in Padova, Italy, in 1977. She received the M.S. degree in electronic engineering from the University of Padova in 2001, where she is currently pursuing the Ph.D. degree.

Her research areas include PMD, design of low-PMD fibers and WDM high-bit-rate optical systems.

G. Lorenzetto, photograph and biography not available at the time of publication.

P. Minzioni was born in Pavia, Italy, on September 8, 1977. He received the M.S. degree in electronics engineering in 2002 from the University of Pavia, Pavia, Italy, where he is currently pursuing the Ph.D. degree in electronics and computer science engineering.

In 2002, he was with Pirelli Labs Optical Innovation, Milan, Italy. His main research interests are nonlinear fiber optics, optical phase conjugation, and Bragg reflectors.

S. Cascelli, photograph and biography not available at the time of publication.

Michele Guglielmucci was born in Benevento, Italy, in 1950. He received the degree in electrical engineering from the University of Naples, Italy, in 1978.

From 1978 to 1984 he was with ASST (the Telephone Agency of the Ministry of PT) in the branch concerning planning and testing of TLC Exchange Power Plants. In 1985 he joined Istituto Superiore delle Comunicazioni e delle Tecnologie dell'Informazione, where was appointed as Head of Optical Fibers and Cables Department. Since 1987, he has been a Member of ITU-T SG.6 in which, currently, he is Rapporteur for Q.10/6 (marinized terrestrial cables) and IEC 86 A. He has also been a Member of the Management Committee of study groups approved by the European Commission such as COST 218 and COST 246. Currently, he is a Member of the Management Committee of COST 270.

Luigi Lattanzi was born in Frascati, Rome, Italy, in 1937. He received the engineer degree in electronics from Rome University in 1964.

He joined the Istituto Superiore PT (now ISCTI), the technical and scientific body of the Italian PT Ministry, to work in the field of telephone transmission. Since 1987 he has been Head of the "Transmission Systems on Physical Support" of ISCTI, with responsibility on research, technical standardization, and testing on optical systems. From 1981 to 1992, he was National Coordinator for ITU-T Study Group 15 (Transmission Systems).

Francesco Matera was born in Rome, Italy, on May 1, 1961. He received the laurea degree in electronics engineering from the University La Sapienza, Rome, in 1985.

In 1986, he received a fellowship from Fondazione Ugo Bordoni, Rome, on optical fibers. Since 1988, he has been a Researcher at Fondazione Ugo Bordoni, where he works on nonlinear effects on optical fibers, optical systems, and optical networks. His main works are in the field of the optical transmission systems and optical networks. He is a Member of European COST266 and Scientific Coordinator of European IST ATLAS.

G. M. Tosi Beleffi, photograph and biography not available at the time of publication.

V. Quiring, photograph and biography not available at the time of publication.

W. Sohler, photograph and biography not available at the time of publication.

Hubertus Suche was born in Neukirchen/Sachsen, Germany, in 1951. He received the Diplom-Physiker and Dr.Rer.Nat. degrees in physics from the University of Dortmund, Germany, in 1978 and 1981, respectively.

In 1981, he joined the Fraunhofer Institut fuer Messtechnik, Freiburg, Germany, as a Research Member in the Department of Fiber Optics. Since 1982, he has been with the University of Paderborn, Germany, as Akademischer Oberrat within the Applied Physics group. He is author/coauthor of about 100 journal and conference contributions and of several book chapters.

Dr. Suche is a member of the German Physical Society.

Samo Vehovc received the B.Sc. and M.Sc. degrees from the University of Ljubljana, Slovenia, in 1998 and 2001, both in electrical engineering.

He is on the Faculty of Electrical Engineering at the University of Ljubljana as a Research Engineer. His research work is focused on electronics for optical fiber communications and radio communications.

Matjaz Vidmar received the B.S.E.E., M.S.E.E., and Ph.D. degrees from the University of Ljubljana, Slovenia, in 1980, 1983, and 1992, respectively.

His doctoral degree involved developing a single-frequency GPS ionospheric correction receiver. He is currently teaching undergraduate and postgraduate courses in electrical engineering at the University of Ljubljana. His current research interests include microwave and high-speed electronics ranging from avionics to optical-fiber communications. He is also taking part in amateur satellite projects. He developed high-efficiency VHF and UHF transmitters that were successfully flown in space on the Microsat mission in 1990 and microwave receivers and IF processors that were successfully flown in space on the AMSAT-P3D satellite in 2000.